

# Physical Aging Studies of Semicrystalline Poly(ethylene Terephthalate)

MARTIN R. TANT\* and GARTH L. WILKES,† *Department of Chemical Engineering, Virginia Polytechnic Institute and State University, Blacksburg, Virginia 24061*

## Synopsis

Physical aging of semicrystalline poly(ethylene terephthalate) has been investigated as a function of crystalline content. Stress-strain, stress relaxation, and differential scanning calorimetry experiments were used to monitor the physical aging process. Both the overall extent and the rate of physical aging in this material decrease with increasing crystallinity. Several possible reasons for this behavior are advanced and discussed. It was also found that the drawing behavior of amorphous PET changes significantly as physical aging progresses. Specifically, for samples aged and then elongated, the extent of localized deformation (necking) and associated strain-induced crystallization was greater for samples aged for longer periods of time.

## INTRODUCTION

The importance of the nonequilibrium state of glassy polymers has become increasingly more prominent over the past several years. Glassy polymers in this nonequilibrium condition exhibit quite dramatic structural and property changes upon annealing below the glass transition temperature.<sup>1-10</sup> This observed aging behavior—variously referred to as nonequilibrium behavior, enthalpy or volume recovery, or simply physical aging—is a direct result of the nonequilibrium nature of the glassy state. As a polymer is cooled at a finite rate through the glass transition, the molecules are not able to reach their equilibrium conformation with respect to temperature due to the rapid increase in viscosity and associated decrease in molecular mobility in the  $T_g$  region. As the temperature is further decreased, the polymer molecules are essentially “frozen” into a nonequilibrium state at that same temperature. There is thus a thermodynamic potential or driving force for the molecules to approach the equilibrium state by undergoing further packing. Although the molecular mobility is greatly decreased in the glass as compared to the rubbery region, it remains finite, thus allowing the molecules to approach the equilibrium state corresponding to normal liquidlike packing. The measureable thermodynamic state functions, enthalpy and volume, have been found to decrease with sub- $T_g$  annealing time as the excess enthalpy and volume originally quenched into the system decrease.

Associated with this approach toward the equilibrium state, there occur changes in the mechanical properties of the polymer system.<sup>1,2,8,9</sup> Typical of these changes are an increase in tensile and flexural yield stresses; a decrease in

\* Present address: Material Sciences Branch, Naval Surface Weapons Center, Dahlgren, Virginia 22448.

† To whom correspondence should be sent.

impact strength, fracture energy, ultimate elongation, and creep rate; and a transition from ductile behavior to brittle fracture. The utilization of polymers as engineering materials requires that the nature and extent of these changes in properties be fully understood. Almost all experimental work reported in the literature has been conducted on purely glassy linear homopolymers. Although it had been previously established that network glassy epoxies undergo physical aging,<sup>2</sup> it was only recently that the first systematic studies of physical aging in these network systems and rubber-modified derivatives were completed.<sup>11,12</sup>

Since nonequilibrium behavior has been observed to occur in covalently crosslinked systems, it may be asked whether similar behavior occurs in "pseudo" network systems such as semicrystalline polymers, where the crystalline regions serve as physical crosslinks, and in partially glassy domain-forming block copolymers, where the glassy regions may also serve as physical crosslinks. Of course, the glassy phase in these materials would be expected to undergo the same changes it would experience if isolated, i.e., as a purely glassy material. However, the important questions which must be asked are whether or not the property changes in the glassy phase result in observable property changes in the two-phase material and, if so, to what extent do these changes occur and how do they relate to the concentration of glassy polymer.

One study has demonstrated that semicrystalline polymers undergo physical aging,<sup>2</sup> but there has been no report of a systematic physical aging study with respect to the variable of crystalline content. Certainly, one would expect that increasing the crystallinity would decrease the overall extent of physical aging, since there would be less glassy amorphous material to undergo this process. In this article, we report results of an investigation on the physical aging of semicrystalline poly(ethylene terephthalate) as a function of the degree of crystallinity. The results of this study are considered important due to the widespread use of this material. Results of a similar study on block copolymers are reported elsewhere.<sup>13,14</sup>

## EXPERIMENTAL

### Materials

Amorphous films of poly(ethylene terephthalate) (PET) supplied through the courtesy of Dr. G. Adams of E. I. du Pont de Nemours and Co. were crystallized by heating under vacuum at various temperatures to induce different levels of crystallinity. Table I shows the levels of crystallinity obtained, along with the time and temperature of crystallization for each. Crystallinity determinations were made with a density gradient column containing an ethanol-carbon tetrachloride mixture.<sup>15</sup> Crystallinities were calculated by taking the density of the perfect PET crystal to be 1.455 g/cm<sup>3</sup> and that of amorphous PET to be 1.335 g/cm<sup>3</sup>.<sup>16</sup> The density measurements were consistently made within 10 min after cooling because of the rather significant changes in density, attributable to nonequilibrium behavior, that occur upon sub- $T_g$  annealing. For example, using the density values stated above, amorphous PET has a density corresponding to 0% crystallinity immediately after quenching; but as free volume decreases and density increases upon sub- $T_g$  annealing, this method shows an

TABLE I  
Crystallization Conditions for PET

Crystallization temperature, °C	Crystallization time, h	Percent crystallinity by density
102	12	12
102	48	22
113	3	29
163	24	39
205	24	51

apparent crystallinity of as much as 3–5%. This effect was also observed for semicrystalline PET but, of course, to a lesser extent. As the crystalline fraction increases, the degree of density change upon sub- $T_g$  annealing is diminished due to the decreased fraction of glassy material and the increased structural rigidity provided by the crystals. Based upon the results reported here, it should therefore be noted that the density of amorphous PET obtained from the literature is the density of PET in a nonequilibrium state.

### Methods

Three characterization techniques were used to follow changes in the mechanical and thermal properties of the PET materials. Stress-strain, stress relaxation, and differential scanning calorimetry experiments were performed as a function of sub- $T_g$  annealing time.

All stress-strain experiments were performed on an Instron model 1122, and stress relaxation experiments were performed on a Tensilon model UTM-II (Toyo Measuring Instruments Co. Ltd.). Dog bone-shaped samples were cut from films of PET of various crystallinities. The dimensions of these samples were 10.00 mm (length) by 2.80 mm (width) by 0.31 mm (thickness). The linear portion of these materials measured 5.75 mm. This was the initial sample length used to calculate percent elongation, since most of the strain occurs in this region.

The amorphous and semicrystalline PET samples were heated to a temperature above their  $T_g$  and annealed at that temperature for a period of 10 min to erase any previous aging. This annealing temperature was 92°C for the amorphous material, but the semicrystalline PET samples were heated to higher temperatures due to the broadening of the glass transition with increasing crystallinity. These temperatures were: 102°C for the 12 and 22% crystalline materials and 132°C for the 29, 39, and 51% crystalline materials. Density measurements confirmed that no change in crystallinity had occurred as a result of this 10-min thermal treatment. After the 10 min of annealing above  $T_g$ , the samples were then immediately quenched below  $T_g$  in an ice-water bath, removed, immediately dried, and then stored at room temperature under atmospheric conditions. Stress-strain and stress relaxation experiments were performed on the amorphous and semicrystalline PET samples as a function of sub- $T_g$  annealing time. The stress-strain experiments were all performed at a crosshead speed of 1 mm/min. For the stress relaxation experiments, the samples were elongated to 0.65% at a crosshead speed of 2 mm/min. The percent

relaxation of stress during the first 10 min of the experiment was calculated for each sample. It was realized that although the macroscopic strain was the same for all stress relaxation experiments, the local strain in the glassy amorphous regions may vary with percent crystallinity, thus possibly contributing to variations in the rate of stress relaxation.

Differential scanning calorimetry experiments were performed on amorphous and 12% crystalline PET to determine the basic qualitative features of the enthalpy recovery process in these materials. A Perkin-Elmer DSC-2 instrument was used for these studies. DSC scans were made with a 10°C/min heating rate. Each sample was scanned through its glass transition, annealed at about 20°C above the  $T_g$  for 5 min, cooled rapidly, and then scanned again. This second scan was taken as the DSC trace of a quenched, unannealed sample.

## RESULTS AND DISCUSSION

### Stress Relaxation

Stress relaxation data for amorphous and 22% crystalline PET are shown in Figures 1 and 2, respectively. It is clear that percent stress relaxation during the first 10 min of the experiment decreases with sub- $T_g$  annealing time, thus indicating an increase in the molecular relaxation times. This result is expected during physical aging as the decrease in free volume with time results in a corresponding decrease in molecular mobility. This reduced mobility causes molecular relaxations to become slower, thus shifting the relaxation spectrum to longer times as the physical aging process proceeds. Determining the percent relaxation of stress during the first 10 min of relaxation as a function of sub- $T_g$  annealing time is only one method of monitoring this change in the relaxation spectrum.

As can be seen from Figures 1 and 2, the decrease in percent stress relaxation is linear with respect to logarithmic sub- $T_g$  annealing times until an *apparent*

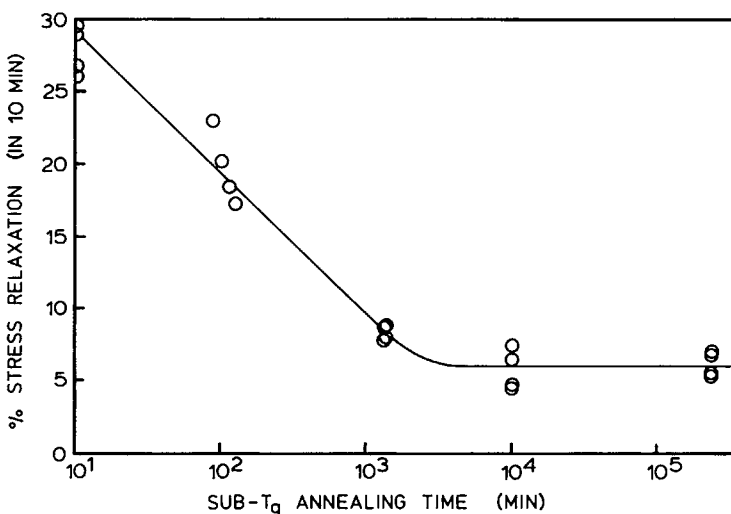


Fig. 1. Percent stress relaxation as function of sub- $T_g$  annealing time for amorphous PET aged at 23°C.

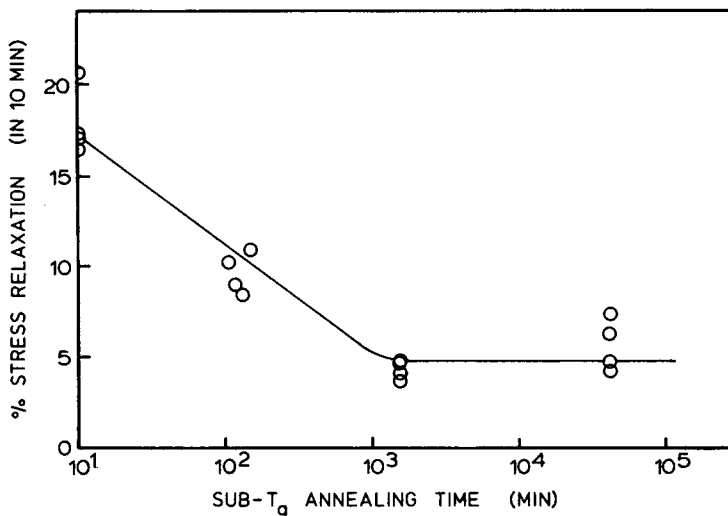


Fig. 2. Percent stress relaxation as function of sub- $T_g$  annealing time for 22% crystalline PET aged at 23°C.

equilibrium value for this experiment at about 2000 min. From the data, one might be tempted to say that an actual equilibrium state has been reached and that physical aging has ceased, but this has proved not to be the case. Matsuoka et al.<sup>8</sup> obtained stress relaxation data for polystyrene aged below  $T_g$  for different times, as is shown in Figure 3. These curves show very little variation during the first part of the stress relaxation experiment. However, as the experiment proceeds, the data for the different annealing times deviate greatly, with the more annealed sub- $T_g$  samples relaxing much more slowly than the samples which had been aged for shorter times. The first part of the curves are seen to approach a single curve (at short relaxation times), while for longer times the respective curves show different behavior.

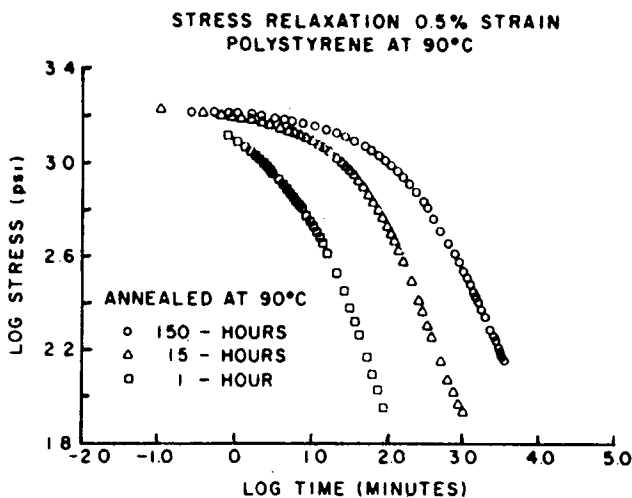


Fig. 3. Stress relaxation in PS with various thermal histories but at the same strain and same temperature.<sup>9</sup>

Thus, it is expected that an apparent equilibrium value of percent stress relaxation during the first few minutes of the stress relaxation experiment would be observed for these polystyrene samples annealed for longer periods of time. This is exactly what has been observed for PET in the present work. To further substantiate this explanation, stress relaxation experiments were performed on two amorphous PET samples which had been annealed below  $T_g$  for different times. It was found that the percent stress relaxation in 10 min was the same for both samples; but as the stress relaxation experiment proceeded, the results were very different, with the older sample relaxing at a much slower rate than the sample which had been annealed for a shorter time period. The results of this experiment are shown in Figure 4, where the calculated percent relaxation of stress is plotted vs. time since the beginning of the stress relaxation experiment (relaxation time). It is clear that had a longer time "window" than 10 min been used to determine the percent stress relaxation, the apparent equilibrium at 2000 min would not have occurred—at least until a longer annealing time had been reached. Thus, the apparent equilibrium obtained at about 2000 min is simply a consequence of the experiment and does *not* indicate that an equilibrium condition has been reached and that physical aging has stopped.

A composite presentation of the stress relaxation data for amorphous PET and the various degrees of semicrystalline PET is given in Figure 5. In general, these curves move to lower values of percent stress relaxation with an increasing degree of crystallinity. The fact that the curve for the 22% crystalline PET lies below the curve for the 29% crystalline PET is likely due to scatter in the data. The slopes of these lines may be related to the rate of recovery toward equilibrium or the rate of physical aging. For discussion purposes, the recovery rate is defined here as being the *negative* of the slope for the percent stress relaxation vs. logarithmic annealing time plot.

Figure 6 shows this recovery rate as a function of crystallinity for PET. The change in recovery rate with percent crystallinity is significant, as the recovery rate of amorphous PET is more than twice that of 51% crystalline PET. The decrease in recovery rate with increasing percent crystallinity may occur for several different reasons. First, as crystallinity increases, the amorphous fraction

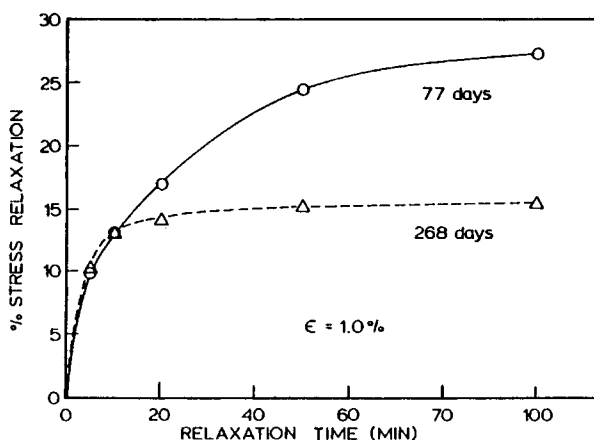


Fig. 4. Percent stress relaxation in amorphous PET with different thermal histories as function of relaxation time, at the same strain and temperature.

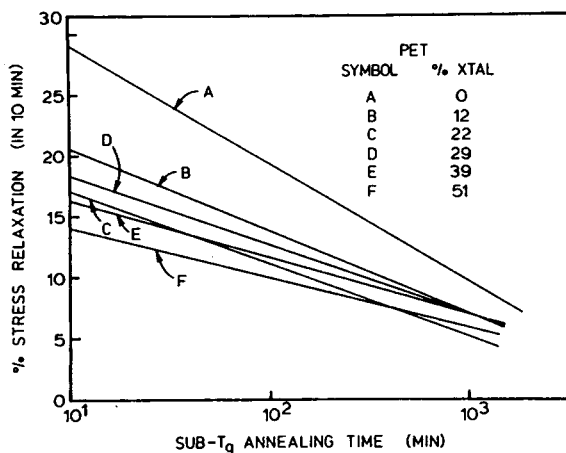


Fig. 5. Composite plot of percent stress relaxation as function of sub- $T_g$  annealing time for PET of various degrees of crystallinity.

decreases, thereby affecting the degree of stress relaxation accordingly. Secondly, broadening of the glass transition with increasing crystallinity would effectively increase the temperature increment below  $T_g$  and thus retard the aging process. Thirdly, the local strain in the glassy amorphous regions may vary as a function of crystallinity, thus altering the rate of stress relaxation.<sup>9</sup> Finally, the crystalline regions may well alter the relaxation spectrum as a result of increasing the rigidity of the overall structure and decreasing the mobility of amorphous molecules that extend into and become part of the crystals. Likely more than one of the above mechanisms contribute to the aging process.

The nonequilibrium phenomenon is an inherent feature of glassy materials and is not observed in crystalline materials. For a totally crystalline polymer, then, one would not expect physical aging to occur, and indeed the recovery rate, as defined here, would be zero. While the extrapolation of the data to 100% crystallinity is great, it is strikingly found that, as shown by the dashed line in Figure 6, this extended line provides a zero recovery rate at 100% crystallinity. This of course is precisely where the physical aging process would be expected to cease.

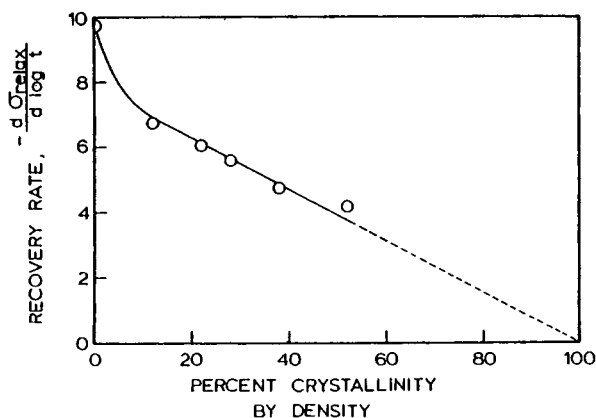


Fig. 6. Recovery rate ( $-d \log \text{relax} / d \log t$ ) for PET as function of percent crystallinity, showing extrapolation to 100% crystallinity.

The recovery rate for amorphous PET does not fall on the linear line formed by data from PET of various crystallinities, as shown in Figure 6. This result might have been expected. Amorphous and crystalline polymers differ greatly in structure, and the properties displayed by these two types of materials are vastly different. Thus, when even a small amount of crystallinity is introduced into an amorphous polymer, the resulting properties and associated relaxation processes are significantly influenced by the crystalline regions. The fact that the recovery rate for amorphous PET is not collinear with the recovery rates for semicrystalline PET materials is therefore not surprising.

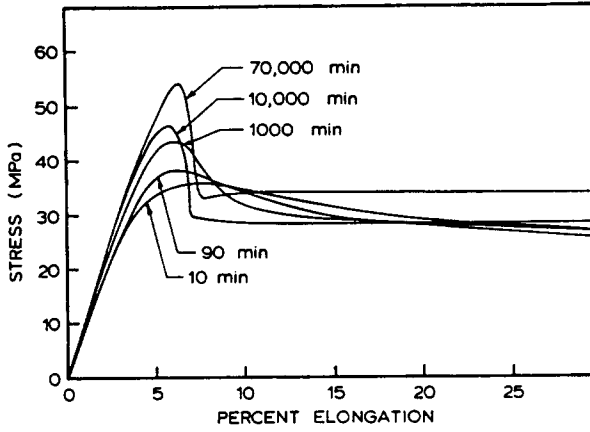
### Stress-Strain Behavior

Stress-strain curves for amorphous PET and PET materials of various crystallinity are shown in Figures 7(a)-(d) as a function of sub- $T_g$  annealing time. Clearly, there is an increase in both Young's modulus and yield stress as well as a decrease in yield strain as physical aging progresses for PET of crystallinities ranging from 0 to 39%. Somewhat similar behavior has been observed for amorphous PET by Petrie<sup>1</sup> and Minnini et al.<sup>17</sup>

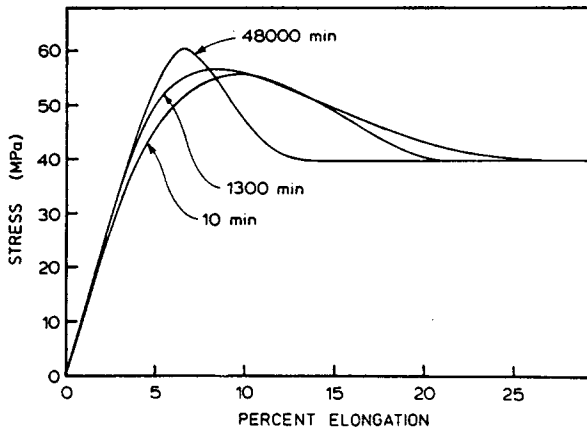
There is no observable change with sub- $T_g$  annealing in the stress-strain behavior of 51% crystalline PET. Again, the increase in Young's modulus is due to the shifting of the relaxation spectrum to longer times, i.e., as free volume and molecular mobility decrease when the material is aged, molecular arrangement mechanisms become progressively slower due to the increased time required for these rearrangements to occur. Thus, when samples annealed below  $T_g$  for a short time are stretched, their comparatively higher molecular mobility allows more rapid rearrangement of the polymer molecules in reducing stress, and thus stress increases at a slower rate. When samples annealed below  $T_g$  for longer times are stretched at the same rate, reduction of stress by molecular rearrangement is slower, and thus stress increases at a faster rate. The increase in yield stress with sub- $T_g$  annealing occurs because, as molecular mobility is decreased upon annealing, a greater amount of energy is necessary to initiate the molecular motions associated with yielding. The fact that stress-strain behavior of 51% crystalline PET does not change upon sub- $T_g$  annealing is clearly due to the high crystallinity involved. As the 51% crystalline sample is stretched, the stress distribution is apparently rather concentrated in the interconnected crystalline regions due to their high resistance to deformation. Thus, changes in the amorphous regions due to physical aging apparently have an insignificant effect on the stress-strain behavior of 51% crystalline PET at the strain rate used for this experiment.

While performing the stress-strain experiments on amorphous PET, another interesting observation was made. Figure 8 shows dog bone samples of amorphous PET that were annealed at room temperature for various times and then elongated 35% (engineering strain) at a crosshead speed of 1 mm/min. There is an obvious difference in optical clarity in the drawn region for samples annealed for different times. It has been demonstrated by wide-angle X-ray scattering (WAXS) that the increased whitening in the drawn region with sub- $T_g$  annealing is due to increased crystallinity (see Fig. 9). Thus, strain-induced crystallinity at 35% elongation, for samples aged for various times and then elongated, increases with sub- $T_g$  annealing time. This is probably due to the decrease in free

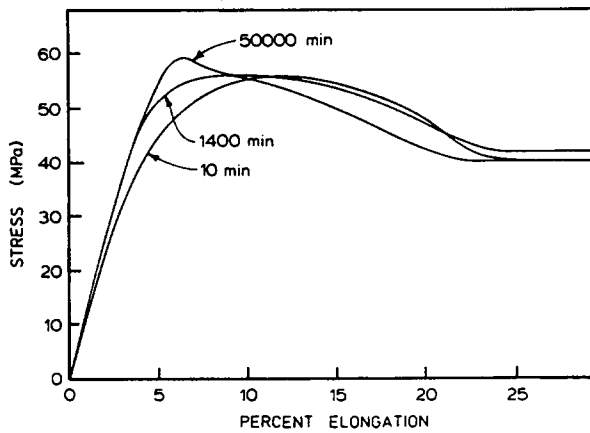




(a)



(b)



(c)

Figure 7. Stress-strain curves measured at various sub- $T_g$  annealing times (a) for amorphous PET, (b) for 22% crystalline PET, (c) for 29% crystalline PET, and (d) for 39% crystalline PET.  $T_A = 23^\circ\text{C}$ .

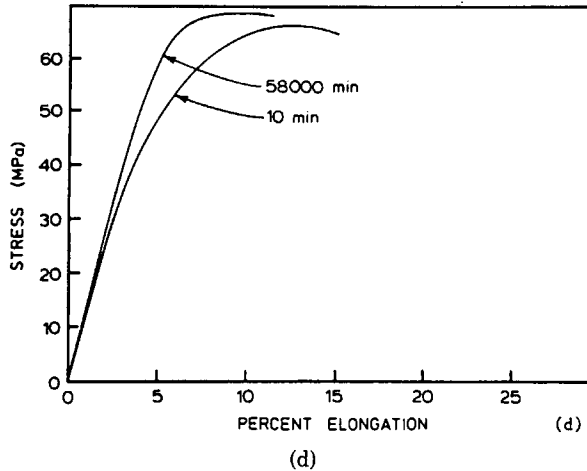


Fig. 7. (Continued from previous page.)

volume upon annealing, i.e., the closer proximity of the molecules in aged samples may possibly promote necking and associated crystallization upon orientation. Further work will be necessary to prove or disprove this speculation.

### Differential Scanning Calorimetry

DSC data for amorphous and 12% crystalline PET are shown in Figures 10 and 11. Figure 10 shows that, in addition to increasing in size, the endothermic enthalpy recovery peak begins well below  $T_g$  and shifts toward  $T_g$  with sub- $T_g$  annealing time. This has been explained on the basis of free volume and molecular mobility.<sup>1</sup> As the temperature of the polymer material is increased during the DSC scan, the enthalpy increases in a manner typical of a solid. When the molecular mobility becomes sufficient, the equilibrium amorphous conformation is rapidly approached, and this is reflected by an absorption of energy—the enthalpy recovery peak. The temperature at which this critical molecular mobility is reached is dependent upon both the availability of free volume necessary for

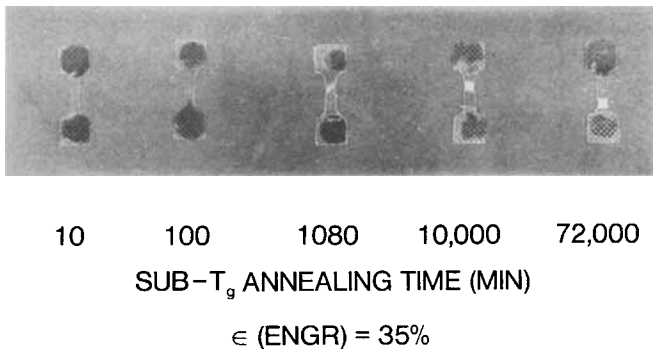


Fig. 8. Drawn amorphous PET elongated at various times after the quench, showing increasing whitening of the drawn region.

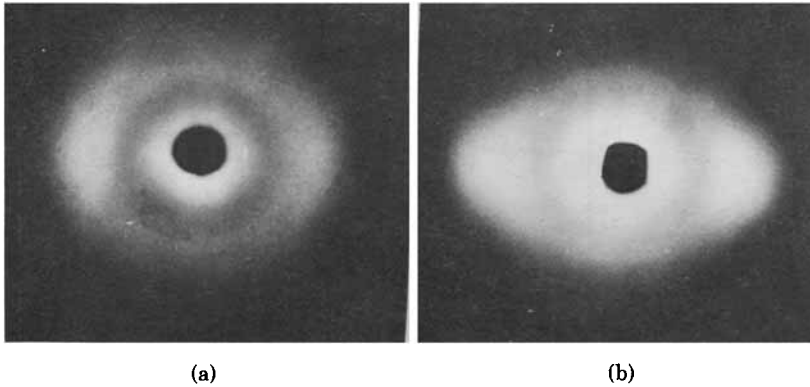


Fig. 9. WAXS patterns of cold-drawn PET having macroscopic elongation of 35%: (a) sub- $T_g$  (23°C) aging = (a) 10 min, (b) 56,000 min.

molecular mobility and the heating rate. However, the degree of free volume is dependent upon the aging history of the material.

As stated earlier, as sub- $T_g$  annealing time increases, the free volume related to molecular mobility decreases, and thus the temperature at which the molecular rearrangement occurs will increase with annealing time since more thermal energy will be required to cause motion. Also, the enthalpy recovery peak will occur at higher temperatures for faster heating rates.<sup>18</sup> This is also explained on the basis of molecular mobility. As an aged material is heated, different relaxation processes begin at different temperatures. At faster heating rates, some of these processes occur more slowly than the rate of change of temperature. Thus, their effect on the DSC trace, the enthalpy recovery peak, is observed at higher temperatures. At slower heating rates, the effects of these processes are observed much closer to the temperature at which they were initiated.

Petrie<sup>19</sup> has also studied the enthalpy recovery behavior of amorphous PET but did not observe a substantial shifting of the recovery peak to higher tem-

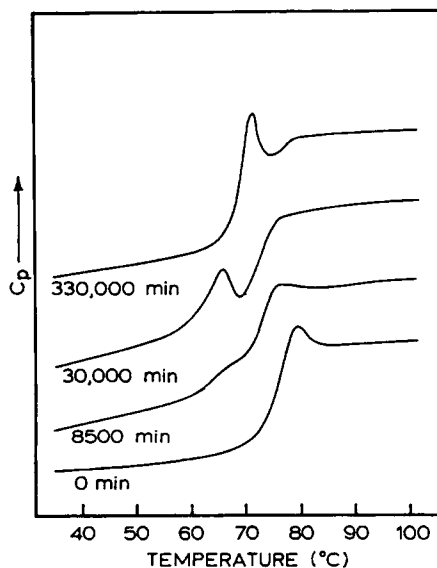


Fig. 10. Annealing time effects on the DSC traces of amorphous PET.  $T_A = 23^\circ\text{C}$ .

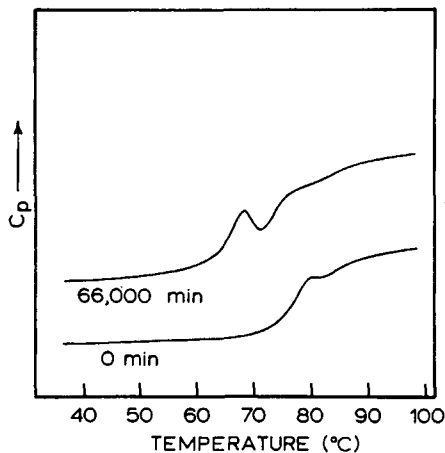


Fig. 11. Annealing time effects on the DSC traces of 12% crystalline PET.  $T_A = 23^\circ\text{C}$ .

peratures. However, Petrie's annealing study was conducted at  $65^\circ\text{C}$ , just below the  $T_g$ , while annealing for this work was conducted at  $23^\circ\text{C}$ . The enthalpy recovery peak would not be expected to occur below the annealing temperature, and thus the fact that it occurs at  $T_g$  when annealed at  $65^\circ\text{C}$  is not surprising. The position of the endotherm is dependent upon the initial state of the glass, as described before, and materials annealed at different temperatures should certainly be expected to be in different states. This shifting of the endotherm to higher temperatures, beginning well below  $T_g$ , has also been observed in undrawn PET fibers by Mitsubishi and Kuroda.<sup>20</sup>

Figure 11 shows that enthalpy recovery also occurs for 12% crystalline PET. This behavior was expected due to the high percentage of glassy polymer present, but it was not previously known whether or not enthalpy recovery would be easily detectable in this semicrystalline polymer by the DSC technique.

## CONCLUSIONS

Both the extent and rate of physical aging in PET were found to decrease with increasing percent crystallinity, as was expected. The recovery rate of semicrystalline PET was determined to be related to percent crystallinity in a linear fashion above 20% crystallinity, with this line extrapolating to zero recovery rate at 100% crystallinity.

The drawing behavior of amorphous PET was found to depend greatly upon the aging history. After aging for different periods of time and then elongating 35%, the drawn region is increasingly more opaque for longer-aged samples. This was found to be due to a higher crystallinity in the drawn region for more-aged samples, apparently due to the increase in packing density which may possibly promote crystallization upon orientation.

Enthalpy recovery behavior was observed in both amorphous and semicrystalline PET, supporting the finding that physical aging occurs in semicrystalline as well as amorphous polymers.

The authors wish to acknowledge the financial support of this work from ONR Grant No. N00014-78-C-0629 and the partial support of ICI Americas, Inc.

## References

1. S. E. B. Petrie, in *Polymeric Materials: Relationships Between Structure and Mechanical Behavior*, Am. Soc. for Metals, Metal Park, OH, 1975.
2. L. C. E. Struik, *Physical Aging in Amorphous Polymers and Other Materials*, Elsevier, New York, 1978.
3. A. J. Kovacs, J. M. Hutchinson, and J. J. Aklonis, in *The Structure of Noncrystalline Materials*, P. H. Gaskell, Ed., Taylor and Francis, London, 1977.
4. E. Ito, K. Yamamoto, Y. Kobazashi, and T. Hatakeyama, *Polymer*, **19**, 39 (1978).
5. S. G. Brown, R. E. Witlan, M. J. Richardson, and N. G. Savill, *Polymer*, **19**, 659 (1978).
6. M. J. Richardson and N. G. Savill, *Polymer*, **18**, 413 (1977).
7. R. E. Robertson, *J. Polym. Sci. Polym. Symp.*, **63**, 173 (1978).
8. S. Matsuoka and H. E. Bair, *J. Appl. Phys.*, **48**, 4058 (1977).
9. S. Matsuoka, H. E. Bair, S. S. Bearder, H. E. Kern, and J. T. Ryan, *Polym. Eng. Sci.*, **18**, 1073 (1978).
10. J. M. O'Reilly, *Polym. Prep. Am. Chem. Soc. Div. Polym. Chem.*, **20**(1), 762 (1979).
11. Z. H. Ophir, J. A. Emerson, and G. L. Wilkes, *J. Appl. Phys.*, **49**, 5032 (1978).
12. J. Kaiser, *Macromol. Chem.*, **180**, 573 (1979).
13. M. R. Tant and G. L. Wilkes, *Polym. Prep. Am. Chem. Soc. Div. Polym. Chem.*, **20**(2), 535 (1979).
14. M. R. Tant and G. L. Wilkes, *Polym. Eng. Sci.* (to appear).
15. B. Wunderlich, *Macromolecular Physics*, Vol. 1, Academic, New York, 1973, p. 382.
16. R. De P. Daubery and C. W. Bunn, *Proc. Roy. Soc.*, **A226**, 531 (1954).
17. R. M. Mininni, R. S. Moore, J. R. Flick, and S. E. B. Petrie, *J. Macromol. Sci. Phys.*, **B8**, 343 (1973).
18. S. G. Brown, R. E. Wetton, M. J. Richardson, and N. G. Savill, *Polymer*, **19**, 659 (1978).
19. S. E. B. Petrie, *J. Polym. Sci., Part A-2*, **10**, 1255 (1972).
20. Y. Mitsuishi and Y. Kuroda, *Sen-i Gakkaishi*, **24**, 11 (1968).

Received May 5, 1980

Accepted February 12, 1981